

Liver segmentation using marker controlled watershed transform

Kiran Malhari Napte, Anurag Mahajan

Department of Electronics and Telecommunication, Symbiosis Institute of Technology, Symbiosis International (Deemed University), SIU, Lavale Pune, India

Article Info

Article history:

Received Mar 30, 2022

Revised Sep 20, 2022

Accepted Oct 15, 2022

Keywords:

Computer tomography

Gaussian filtering

Image enhancement

Liver segmentation

Watershed transform

ABSTRACT

The largest organ in the body is the liver and primarily helps in metabolism and detoxification. Liver segmentation is a crucial step in liver cancer detection in computer vision-based biomedical image analysis. Liver segmentation is a critical task and results in under-segmentation and over-segmentation due to the complex structure of abdominal computed tomography (CT) images, noise, and textural variations over the image. This paper presents liver segmentation in abdominal CT images using marker-based watershed transforms. In the pre-processing stage, a modified double stage gaussian filter (MDSGF) is used to enhance the contrast, and preserve the edge and texture information of liver CT images. Further, marker controlled watershed transform is utilized for the segmentation of liver images from the abdominal CT images. Liver segmentation using suggested MDSGF and marker-based watershed transform help to diminish the under-segmentation and over-segmentation of the liver object. The performance of the proposed system is evaluated on the LiTS dataset based on Dice score (DS), relative volume difference (RVD), volumetric overlapping error (VOE), and Jaccard index (JI). The proposed method gives (Dice score of 0.959, RVD of 0.09, VOE of 0.089, and JI of 0.921).

This is an open access article under the [CC BY-SA](https://creativecommons.org/licenses/by-sa/4.0/) license.



Corresponding Author:

Anurag Mahajan

Department of Electronics and Telecommunication, Symbiosis Institute of Technology, Symbiosis International (Deemed University)

Pune, Maharashtra, India

Email: anurag.mahajan@sitpune.edu.in

1. INTRODUCTION

The liver is the third and seventh cause of causality due to cancers across the globe. In 2020 it is estimated that 30,230 and 9,930 males and females are died due to liver cancer. The liver cancer rate is steadily increasing by 2% since 1970 [1]. The largest organ in the human body, the liver, is situated on the right side of the abdomen. The liver's primary job is to filter blood coming from the digestive system before it is sent to the rest of the body. It also helps in the metabolism and detoxification of chemicals and drugs. The liver also produces proteins that are important for blood clotting [2].

Primary and secondary liver cancers are the two subtypes of liver cancer. Primary liver cancer is brought on by deviations in the various liver cells [3]. Primary liver cancers are categorized as hepatocellular carcinoma (HCC), intrahepatic cholangiocarcinoma, hemangiosarcoma, angiosarcoma, and hepato-blastoma [4]. HCC is most general and accounts for 75% of all liver cancers. Secondary liver cancer originates due to the cells from other body parts such as the stomach, lungs, breast, colon, and pancreas. Secondary liver cancers are also called metastatic liver cancer [5]. Liver cancer may cause due to heavy alcohol use, smoking, family history, obesity diabetes, hepatitis B or C virus, and low immunity. Some of the common symptoms

of liver cancers are abdominal pain, weight loss, jaundice, abdomen swelling, nausea, fatigue, back pain, vomiting, fever, or itching [6]. Figure 1 shows the liver anatomy in Figure 1(a), normal liver computed tomography (CT) image in Figure 1(b), and liver cancer CT images in Figure 1(c).

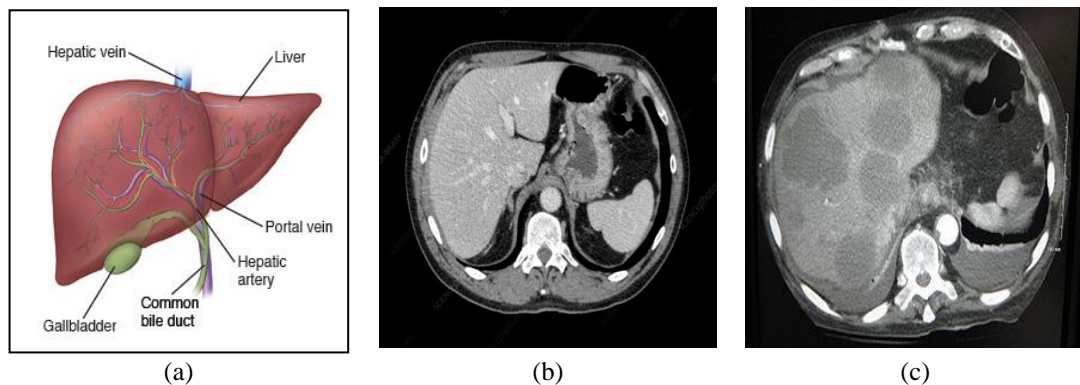


Figure 1. The liver anatomy: (a) liver structure, (b) normal liver CT image, and (c) liver cancer CT image

Liver cancer is more common in males compared to females and in people over age so. Liver cancer can be diagnosed by measuring bilirubin, enzymes, and proteins alpha-protein (AFP) in blood, and through liver biopsy. In the early years, liver cancer analysis used to be performed using various manual tests such as cytotoxic chemotherapy, immunotherapy, or oncolytic virus therapy [7]. Liver segmentation plays vital role in the liver tumor detection in the computer vision. However, due to the liver's uneven and excessive segmentation in the abdomen CT scans, tumor segmentation is difficult. Many times, because of inadequate segmentation the borderline liver tumor detection is challenging. Thus, there is need to focus on the liver segmentation to improve the liver cancer detection.

Computer vision-based biomedical image processing has attracted the attention of researchers toward liver cancer segmentation and detection using various images such as ultrasonic images magnetic resonance imaging (MRI), single-photon emission computed tomography (SPECT), and positron emission tomography (PET). CT scan is a faster method of capturing biomedical images and it can give images of tissues, skeletal structure, and organs. Thus, CT images are widely used for the analysis of abdominal parts of the body. Liver segmentation in the abdominal CT images is a critical task because of a low contrast between variable liver areas and the neighboring organs such as the stomach, kidney, pancreas, and muscles [8], [9]. Abdominal CT images consist of various body parts along with the liver. To extract the correct properties of the liver, the liver portion of the CT images must be segmented. In the past, a variety of ways for separating the liver from abdominal CT scans have been reported. These techniques can be divided into three categories: intensity-based, structure-based, and machine learning or deep learning techniques.

This paper presents, effective liver segmentation using a modified double stage gaussian filter (MDSGF) for liver image enhancement and a marker-controlled watershed algorithm for liver segmentation. The objectives of the paper are summarized as follows: i) Implementation of proposed MDSGF for liver image enhancement to tackle the problem of noise, and complex structure of the abdominal region; ii) Implementation of marker controlled watershed algorithm for liver segmentation to analyze the effect of proposed enhancement on the segmentation; and iii) Performance evaluation of proposed scheme on the LiTS dataset based on dice score (DS), volume overlapping error, relative volume difference, Jaccard index.

The remaining paper is structured as follow: section 2 focuses on the related work on liver segmentation based on various computer vision based techniques. Section 3 gives a brief discussion of the proposed methodology that encompasses the pre-processing and segmentation of liver CT image. Section 4 provides the experimental results and discussion of liver cancer detection. Finally, section 5 concludes the paper and gives the future direction for the improvement of the work.

2. LITERATURE REVIEW

Various computer vision based methods have been presented for the liver segmentation in last two decades. The intensity-based techniques are the active contour model [10], region growing technique [11], super-pixel technique [12], graph cut method [13], clustering-based techniques [14], and machine learning-based techniques. Intensity-based techniques consider the gray intensity value of the pixel with the

neighborhood pixel intensity to decide the texture of the liver. In the techniques, the seed points are manually placed by the expert in the liver parenchyma. The pixel that matches with the seed pixels is clustered collectively to form the homogeneous texture region. Because the shape control capability was not available, intensity-based approaches frequently produced leakage in the manually seeded area, rough ridges, and edges. Intensity-based approaches have been found to be ineffective for magnetic resonance pictures with very diverse textures [15]. In the graph-cut technique, the liver part is roughly considered as the foreground and the peri-hepatic structure is considered as the background part. Then using cut methods the foreground and background pixels are separated into the homogeneous regions [16]. Machine learning-based methods such as support vector machines (SVMs) and artificial neural networks (ANN) [15] have been successfully presented for the quantitative feature extraction of the image texture. Recently, deep learning has attracted the wide attention of researchers for medical image segmentation because of its higher discriminative power, representation capability, and internal connectivity. Fan *et al.* [17] presented multi-scale context nested UNet (MSN-Net) for the liver segmentation to diminish the gradient vanishing problem and lessen the semantic gap. It consists of a multi-scale context fusion network that combined high and low-level features to improve increases the complexity of the network. Bai *et al.* [18] presented a multi-scale candidate generation method (MCG), 3D fractal residual network (3D FRN), and an active contour model (ACM) to deal with varying size, shape, and location of the tumor. It suffered from accurate detection of multiple tumor regions separately and borderline tumors. Li *et al.* [19] investigated hybrid densely connected UNet (H-DenseUNet) for accurate and automatic HCC detection. The use of parallel training makes the system extremely complex. Wang *et al.* [20] investigated the hybrid dilated and attention residual-UNet (HDA-ResUNet) for the contextual liver segmentation. It showed DS, of 0.94 but suffers from poor balancing of computational resources and spatial dimensions. DL-based algorithms have given better performance and highly discriminative capability than the intensity-based methods. The performance of DL-based techniques is highly dependent on noise, contrast, shape, structure, borders, and the type of imaging technique for the liver image.

Watershed transform is a region-based segmentation technique based on mathematical morphology and geographical information of the image. Watershed transform has attracted wide attention towards medical image segmentation because of its simplicity, lesser computational steps, and ability to segment smaller as well as larger objects in the image. The traditional watershed algorithm often results in over-segmentation of the objects in medical images. To minimize the over-segmentation of the liver in medical magnetic resonance (MR) images, Lawankar *et al.* [21] investigated a marker watershed transform algorithm for the liver segmentation along with a Weiner filter for noise removal in images. It has given poor performance because of the spatial invariance of the Weiner filter. Abdallah [22] has shown that marker-controlled watershed transformation can work better in presence of speckle noise and can eliminate the problem caused due to contrast and boundaries of the liver. Huynh *et al.* [23] proposed a watershed algorithm for liver segmentation and an active contour model for refinement of the segmentation. Anter *et al.* [24] presented an adaptive watershed transform for the liver tumor segmentation that tackles the problem of high noise, large variance, and fuzziness due to the same intensity regions of the tumor. They have used neutrosophic sets (NS), and fast fuzzy c-mean clustering algorithms (FFCM) along with watershed transform to improve the segmentation results. They have used a smaller dataset for the experimentation whereas the results for the larger dataset were not explored. Watershed-based algorithms have given the better performance and highly discriminative capability than other segmentation techniques. Very few researchers have given concentration on the enhancement and filtering of liver CT images which limits the performance of the liver segmentation in noisy and high contrast images. Sometimes, these techniques may result in leakage or coarse segmentation due of the noise and rotation. Still, there is scope for improvement in the watershed algorithm to avoid over-segmentation and to reduce the noise effect [25]–[27].

3. PROPOSED METHOD

The flow diagram of the proposed marker-based watershed transform for the liver segmentation is shown in Figure 2. The proposed system is evaluated on the LiTS dataset which consists of 200 CT volumes with different contrast levels, tissue abnormalities, and liver size [28]. The 2-D images are selected from the specific volume of original CT data having complete view of the all-abdominal organs to minimize the computational efforts.

The pre-processing stage includes the separation of the liver image into three channels such as red, green, and blue. Previous liver segmentation has given very little concentration on the liver image filtering which degrades the performance of the liver segmentation. Nidhyanandhan *et al.* [29] proposed the DSGF, a double stage Gaussian filter for improving underwater images. This method needs visual correction after principal component analysis (PCA) fusion which degrades the edge information of the liver CT images. In this paper, we propose a MDSGF that considers Wavelet transform-based fusion for the liver image enhancement to preserve the edges of the liver CT images as illustrated in Figure 3.

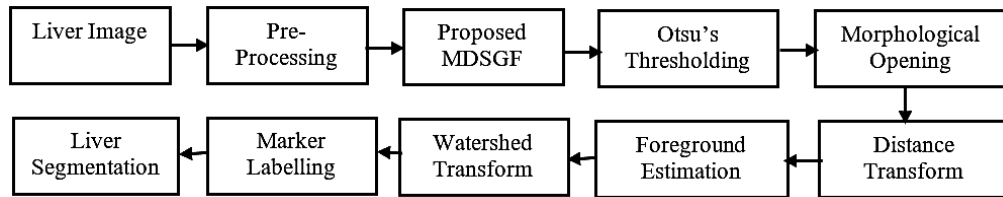


Figure 2. Flow diagram of proposed liver segmentation technique

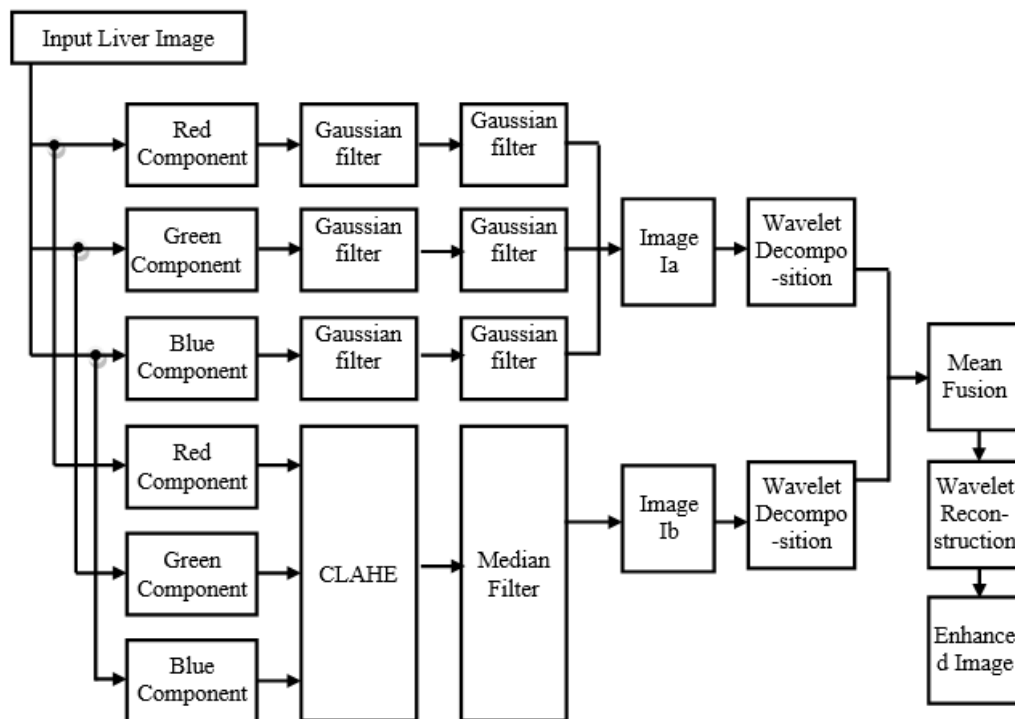


Figure 3. Flow diagram of proposed MDSGF

In the proposed MDSGF, the original liver CT image is separated into red, green, and blue color channels. In the first stage, a Gaussian filter is applied two times for the individual color channel. Gaussian filter is a low pass filter that eliminates the high-frequency components present in the lever CT image. The Gaussian filtering for the two-dimensional liver CT image is shown in (1) [30].

$$G(x, y) = \frac{1}{2\pi\sigma^2} e^{-\frac{x^2+y^2}{2\sigma^2}} \quad (1)$$

where, σ stands for the standard deviation of the Gaussian distribution, x and y represent the position of pixels in the Gaussian window. The Gaussian filter with different window sizes is convolved with the original image to get the smooth borders in the stomach CT image [31]. Three different values of variance (σ) are selected for each channel Gaussian filter. Higher (0.9), low (0.3), and medium (0.5) are selected for the Gaussian filtering of red, green, and blue color channels respectively. In the second phase, contrast limited adaptive histogram is applied to each color channel to enhance the contrast of each color channel. Further, median filtering is applied to smooth the texture of the liver image and minimize the non-uniform components in the liver image. The two images are fused using the Wavelet transform where these images are decomposed into four components such as approximation, diagonal, horizontal, and vertical components. We have used the Haar wavelet filter for the wavelet decomposition. These four components of the two images are combined using the mean fusion method. Then inverse wavelet transform is applied to reconstruct the images to construct the enhanced image. The wavelet transform-based image fusion maintains the quality of edges and textural information of the liver CT image [32].

Using Otsu's thresholding, the grey image is transformed into a binary image. In this method, the image histogram is split into two parts and the threshold is selected where the weighted variance of the regions is minimum [33], [34]. The threshold value is selected using (2).

$$\sigma_w^2(t) = w_1(t)\sigma_1^2 + w_2(t)\sigma_2^2 \quad (2)$$

where, σ_1^2 and σ_2^2 are the variance of the two regions. $w_1(t)$ and $w_2(t)$ are the probabilities of the two classes divided by t which lies between 0 to 255. The binary image obtained using Otsu's thresholding considers the within-class variation over the lower intensity and high-intensity regions. The morphological opening is performed to estimate the background region of the image [35].

The distance transform gives the distance of the pixel from the nearest border. This distance is used to find the peak point and valley points in the image. The distance transform gives the connected components in the image [36], [37].

Any gray-scale image is viewed as a tomographic surface that consists of peak points representing the high-intensity pixels and the valley points representing low-intensity values [38]. Watershed transform is based on filling the water in the isolated valley points which are represented by different label values. When the water level is increased various valley points start to merge. To avoid the merging of these valley regions, the regions are separated by border [39]. The process of water filling and border construction is continued till all the peaks are covered. Watershed segmentation results in over-segmentation due to texture irregularity and noise in the liver image. The marker-based watershed algorithm works on the estimation of the foreground and background region of the image. The watershed transform is applied to the distance transformed image. The marker image consists of the labels for different regions of the liver image. The background region is labeled using 0, the foreground region is labeled with 1, and the border pixels which separate different watershed regions are represented by -1 [40], [41].

4. RESULTS AND DISCUSSION

The proposed system is implemented using Python 3.8 and OpenCV toolbox on the personal computer having a core i3 processor with 2.64 GHz speed, 4 GB RAM, and windows operating system. The visualizations of the various stages of the proposed systems are shown in Figure 4. The outcomes of the proposed liver enhancement and segmentation approach are evaluated on the LiTS dataset that encompasses 200 liver CT images along with its ground truth images. All the images are having dimensions of 512×512 pixels.

Figure 4(a) shows original liver CT image sample from LiTS dataset, Figure 4(b) provides the filtered image using proposed MDSGF, Figure 4(c) shows the binary image output obtained using Otsu's thresholding and Figure 4(d) shows morphologically filtered image with minimize the noise in binary image. The distance transform images shown in Figure 4(e) is used to find peak and valley points to construct watershed image as given in Figure 4(f). Figure 4(g) shows the watershed ridge lines, Figures 4(h) and 4(i) shows the segmented liver region and liver area respectively. It helps to minimize the under and over segmentation of the liver object.

Figure 4 shows that the proposed MDSGF along with marker controlled watershed provides better segmentation of the boundary region of the liver area from the abdominal CT image. It helps to minimize the under and over segmentation of the liver object. The performance of the proposed MDSGF is compared with a simple Gaussian filter and DSGF based on mean square error (MSE), peak signal to noise ratio (PSNR), and structural similarity index measure (SSIM) as provided in (3) to (5). It is found that the proposed MDSGF shows better PSNR, improved SSIM, and lower MSE as given in Table 1.

$$SSIM(x, y) = \frac{(2\mu_x\mu_y+c_1)(2\sigma_{xy}+c_2)}{(\mu_x^2+\mu_y^2+c_1)(\sigma_x^2+\sigma_y^2+c_2)} \quad (3)$$

where, μ_x , μ_y stands for an average of the original and enhanced liver image, μ_x^2 , μ_y^2 stands for the variance of the original and enhanced liver image, σ_{xy} is the covariance of the original and enhanced image, $c_1 = (k_1L)^2$ and $c_2 = (k_2L)^2$ weak denominator stabilizer, L is the dynamic range of liver image pixels (up to 255 for an 8-bit image), $k_1 = 0.01$ and $k_2 = 0.03$. SSIM value ranges between 0 and 1. A larger value of SSIM shows better enhancement of the image. SSIM is calculated over the window size (x, y) of 5×5 pixels.

$$MSE = \frac{1}{mn} \sum_{i=0}^{m-1} \sum_{j=0}^{n-1} [I(i, j) - N(i, j)]^2 \quad (4)$$

$$PSNR = 10 \cdot \log_{10} \left(\frac{2^B - 1}{MSE} \right) \quad (5)$$

where, $I(i, j)$ and $N(i, j)$ are original and enhanced images, m and n stand for rows and columns of images, and B is the number of bits per sample.

Table 1 shows that the proposed system gives SSIM of 0.89, PSNR of 50.34 dB, and MSE of 0.6 for a 3×3 window which is superior to a simple Gaussian filter and DSGF. Increasing the window size diminishes the fine structures in the liver image. The smaller local window (3×3) helps to capture the local variations to distinguish the different objects in the CT image. The higher SSIM shows that the proposed filtering scheme retains the structural content of the CT image that avoids the under or over segmentation of the liver. It has given better performance in terms of SSIM, PSNR and MSE compared with single stage Gaussian filter and DSGF for CT image enhancement.

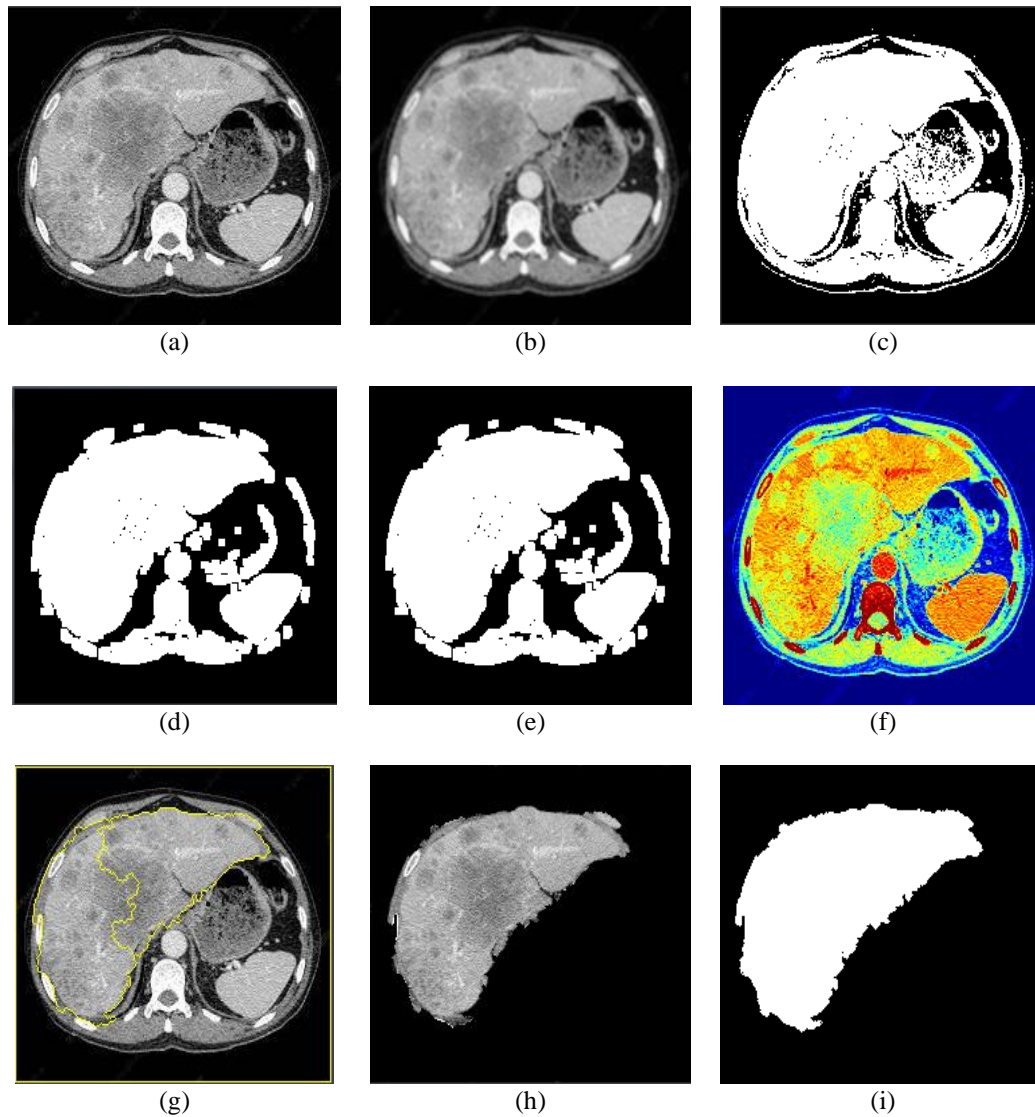


Figure 4. Visualization of experimental results; (a) original image, (b) MDSGF filtered image, (c) Otsu's threshold image, (d) morphological filtered image, (e) distance transform, (f) watershed regions, (g) watershed ridge lines, (h) segmented liver region, and (i) segmented liver area

Table 1. Performance of MDSGF (average value for LiTS dataset)

Method	3×3 Window		
	SSIM	PSNR (dB)	MSE
Gaussian Filter	0.85	49.08	0.8
DSGF	0.87	49.67	0.7
Proposed MDSGF	0.89	50.34	0.6

The performance of the segmentation algorithm is evaluated based on segmentation performance metrics such as DS, volumetric overlapping error (VOE), relative volume difference (RVD), and Jaccard index (JI). The DS, VOE, RVD, and JI are computed using (6) to (9).

$$DS(A, B) = \frac{2|A \cap B|}{|A| + |B|} \quad (6)$$

$$VOE(A, B) = 1 - \frac{|A \cap B|}{|A \cup B|} \quad (7)$$

$$RVD(A, B) = \frac{|A| - |B|}{|B|} \quad (8)$$

$$JI(A, B) = \frac{DS}{2 - DS} \quad (9)$$

where A and B represent the binary mask of the segmented liver and the ground truth image. A smaller value of VOE represents better liver segmentation whereas a higher DS represents better segmentation results. RVD is a measure of segmentation where a positive RVD value refers to over-segmentation whereas a negative RVD value refers to under-segmentation the similarity between the segmented image and the ground truth is measured by JI i.e. Jacard index.

The results of the proposed technique are compared with previous implementations of liver segmentation such as watershed-active contouring [23] and adaptive watershed transform [24]. The performance of the proposed method is also compared with recent deep learning-based liver segmentation techniques such as MSN-Net [17], ACM-ResNet [18], H-DenseUNet [19] and HAD-ResUNet [20]. It is observed that proposed MDSGF helps to increase the liver segmentation by smoothing the irregularities present in the abdominal CT images as shown in Table 2. The proposed technique has shown better improvement in DS and JI respectively over the previous segmentation techniques such as watershed-Active Contouring, adaptive watershed transforms, ACM-ResNet, MSN-Net, HAD-ResUNet and H-DenseUNet. It shows a slightly declined VOE compared with the watershed-active contouring technique and MSN-Net. The use of MDSGF helps to preserve the edge, shape, and texture properties of the liver region help to segment the liver area accurately using marker-controlled watershed transform, and gives a superior improvement in DS, VOE, JI, and RVD respectively over the segmentation without MDSGF.

Table 2. Performance comparison of proposed method

Method	DS	VOE	JI	RVD
ACM-ResNet [18]	0.67	0.324	-	0.194
H-DenseUNet [19]	0.937	0.116	-	-0.010
MSN-Net [17]	0.942	0.04	0.89	-
HAD-ResUNet [20]	0.940	-	0.89	-
Watershed+ Active contouring [23]	0.911	0.083	-	-
Adaptive watershed transform [24]	0.928	-	0.868	-
Proposed method (With MDSGF)	0.959	0.089	0.921	0.09

5. CONCLUSION

Thus, this paper presents automatic computer vision-based liver segmentation using marker-controlled watershed transform. The proposed marker-controlled watershed transform along with the proposed novel modified double stage Gaussian filter tackles the problem of over-segmentation in generalized watershed-based segmentation caused due to noise, complexity in liver structure, and contrast of the liver image. The MDSGF of the CT images has shown improvement in the liver segmentation. The proposed system has shown better performance for liver segmentation in noisy and complex structured abdominal CT images. The Gaussian filter has shown improvement in the liver segmentation performance compared to baseline algorithms. It has demonstrated resilience to both under- and over-segmentation of the liver area on abdominal CT imaging. The proposed method results in a DS of 0.959, VOE of 0.089, JI of 0.921, and RVD of 0.09. The future scope of the proposed work consists of performance improvement of the watershed segmentation technique using deep learning algorithms. Further, the proposed method can be extended for liver tumor detection.

ACKNOWLEDGEMENTS

I would like to thank the Principal, Head of Department (E&TC) of Pimpri Chinchwad College of Engineering and Research, Ravet for their continuous support and motivation for the research.




REFERENCES

- [1] ASCO, "Liver cancer: statistics," cancer.net, 2021. <https://www.cancer.net/cancer-types/liver-cancer/statistics> (accessed May 15, 2021).
- [2] I. M. Arias *et al.*, *The liver: biology and pathobiology*. John Wiley & Sons, 2020.
- [3] M. Torbenson and P. Schirmacher, "Liver cancer biopsy - back to the future?!", *Hepatology*, vol. 61, no. 2, pp. 431–433, Feb. 2015, doi: 10.1002/hep.27545.
- [4] Healthline, "Liver cancer." healthline.com, <https://www.healthline.com/health/liver-cancer> (accessed Apr. 10, 2021).
- [5] D. Sia, A. Villanueva, S. L. Friedman, and J. M. Llovet, "Liver cancer cell of origin, molecular class, and effects on patient prognosis," *Gastroenterology*, vol. 152, no. 4, pp. 745–761, Mar. 2017, doi: 10.1053/j.gastro.2016.11.048.
- [6] Mayo clinic, "Liver cancer." mayoclinic.org, <https://www.mayoclinic.org/diseases-conditions/liver-cancer/symptoms-causes> (accessed Apr. 10, 2021).
- [7] C.-Y. Liu, K.-F. Chen, and P.-J. Chen, "Treatment of liver cancer," *Cold Spring Harbor perspectives in medicine*, vol. 5, no. 9, 2015.
- [8] F. A. Mohammed and S. Viriri, "Liver segmentation: A survey of the state-of-the-art," in *2017 Sudan Conference on Computer Science and Information Technology (SCCSIT)*, Nov. 2017, pp. 1–6, doi: 10.1109/SCCSIT.2017.8293049.
- [9] A. Das, U. R. Acharya, S. S. Panda, and S. Sabut, "Deep learning based liver cancer detection using watershed transform and Gaussian mixture model techniques," *Cognitive Systems Research*, vol. 54, pp. 165–175, May 2019, doi: 10.1016/j.cogsys.2018.12.009.
- [10] A. Hoogi, A. Subramaniam, R. Veerapaneni, and D. L. Rubin, "Adaptive estimation of active contour parameters using convolutional neural networks and texture analysis," *IEEE Transactions on Medical Imaging*, vol. 36, no. 3, pp. 781–791, Mar. 2017, doi: 10.1109/TMI.2016.2628084.
- [11] O. F. Abd-Elaziz, M. S. Sayed, and M. I. Abdullah, "Liver tumors segmentation from abdominal CT images using region growing and morphological processing," in *2014 International Conference on Engineering and Technology (ICET)*, Apr. 2014, pp. 1–6, doi: 10.1109/ICEngTechnol.2014.7016813.
- [12] T. Kitrungrotsakul, X.-H. Han, and Y.-W. Chen, "Liver segmentation using superpixel-based graph cuts and restricted regions of shape constrains," in *2015 IEEE International Conference on Image Processing (ICIP)*, Sep. 2015, pp. 3368–3371, doi: 10.1109/ICIP.2015.7351428.
- [13] G. Li, X. Chen, F. Shi, W. Zhu, J. Tian, and D. Xiang, "Automatic liver segmentation based on shape constraints and deformable graph cut in CT images," *IEEE Transactions on Image Processing*, vol. 24, no. 12, pp. 5315–5329, Dec. 2015, doi: 10.1109/TIP.2015.2481326.
- [14] X. Li, S. Luo, and J. Li, "Liver segmentation from CT image using fuzzy clustering and level set," *Journal of Signal and Information Processing*, vol. 04, no. 03, pp. 36–42, 2013, doi: 10.4236/jsip.2013.43B007.
- [15] N. Sharma *et al.*, "Automated medical image segmentation techniques," *Journal of Medical Physics*, vol. 35, no. 1, p. 3, 2010, doi: 10.4103/0971-6203.58777.
- [16] Y. Chen, Z. Wang, J. Hu, W. Zhao, and Q. Wu, "The domain knowledge based graph-cut model for liver CT segmentation," *Biomedical Signal Processing and Control*, vol. 7, no. 6, pp. 591–598, Nov. 2012, doi: 10.1016/j.bspc.2012.04.005.
- [17] T. Fan, G. Wang, X. Wang, Y. Li, and H. Wang, "MSN-Net: a multi-scale context nested U-Net for liver segmentation," *Signal, Image and Video Processing*, vol. 15, no. 6, pp. 1089–1097, Sep. 2021, doi: 10.1007/s11760-020-01835-9.
- [18] Z. Bai, H. Jiang, S. Li, and Y.-D. Yao, "Liver tumor segmentation based on multi-scale candidate generation and fractal residual network," *IEEE Access*, vol. 7, pp. 82122–82133, 2019, doi: 10.1109/ACCESS.2019.2923218.
- [19] X. Li, H. Chen, X. Qi, Q. Dou, C.-W. Fu, and P.-A. Heng, "H-DenseUNet: hybrid densely connected UNet for liver and tumor segmentation from CT volumes," *IEEE Transactions on Medical Imaging*, vol. 37, no. 12, pp. 2663–2674, Dec. 2018, doi: 10.1109/TMI.2018.2845918.
- [20] Z. Wang, Y. Zou, and P. X. Liu, "Hybrid dilation and attention residual U-Net for medical image segmentation," *Computers in Biology and Medicine*, vol. 134, p. 104449, Jul. 2021, doi: 10.1016/j.compbiomed.2021.104449.
- [21] M. Lawankar, S. Sangewar, and S. Gugulothu, "Segmentation of liver using marker watershed transform algorithm for CT scan images," in *2016 International Conference on Communication and Signal Processing (ICCSP)*, Apr. 2016, pp. 0553–0556, doi: 10.1109/ICCSP.2016.7754200.
- [22] Y. M. Y. Abdallah, "An accurate liver segmentation method using parallel computing algorithm," *Journal of Biomedical Engineering and Medical Imaging*, vol. 2, no. 3, pp. 15–23, Jun. 2015, doi: 10.14738/jbemi.23.1187.
- [23] H. T. Huynh, N. Le-Trong, P. T. Bao, A. Oto, and K. Suzuki, "Fully automated MR liver volumetry using watershed segmentation coupled with active contouring," *International Journal of Computer Assisted Radiology and Surgery*, vol. 12, no. 2, pp. 235–243, Feb. 2017, doi: 10.1007/s11548-016-1498-9.
- [24] A. M. Anter and A. E. Hassenian, "CT liver tumor segmentation hybrid approach using neutrosophic sets, fast fuzzy c-means and adaptive watershed algorithm," *Artificial Intelligence in Medicine*, vol. 97, pp. 105–117, Jun. 2019, doi: 10.1016/j.artmed.2018.11.007.
- [25] M. Ahmad *et al.*, "A lightweight convolutional neural network model for liver segmentation in medical diagnosis," *Computational Intelligence and Neuroscience*, vol. 2022, pp. 1–16, Mar. 2022, doi: 10.1155/2022/7954333.
- [26] W. Tang, D. Zou, S. Yang, J. Shi, J. Dan, and G. Song, "A two-stage approach for automatic liver segmentation with faster R-CNN and DeepLab," *Neural Computing and Applications*, vol. 32, no. 11, pp. 6769–6778, Jun. 2020, doi: 10.1007/s00521-019-04700-0.
- [27] S. Di, Y. Zhao, M. Liao, Z. Yang, and Y. Zeng, "Automatic liver tumor segmentation from CT images using hierarchical iterative superpixels and local statistical features," *Expert Systems with Applications*, vol. 203, Oct. 2022, doi: 10.1016/j.eswa.2022.117347.
- [28] P. Bilic *et al.*, "The liver tumor segmentation benchmark (LiTS)," *arXiv preprint arXiv:1901.04056*, Jan. 2019.
- [29] S. S. Nidhyandhan, R. Sindhuja, and R. S. S. Kumari, "Double stage gaussian filter for better underwater image enhancement," *Wireless Personal Communications*, vol. 114, no. 4, pp. 2909–2921, Oct. 2020, doi: 10.1007/s11277-020-07509-6.
- [30] R. A. Haddad and A. N. Akansu, "A class of fast Gaussian binomial filters for speech and image processing," *IEEE Transactions on Signal Processing*, vol. 39, no. 3, pp. 723–727, Mar. 1991, doi: 10.1109/78.80892.
- [31] H. M. El-Hoseny *et al.*, "An optimal wavelet-based multi-modality medical image fusion approach based on modified central force optimization and histogram matching," *Multimedia Tools and Applications*, vol. 78, no. 18, pp. 26373–26397, Sep. 2019, doi: 10.1007/s11042-019-7552-1.
- [32] M. Nixon and A. Aguado, *Feature extraction and image processing for computer vision*. Academic press, 2019.




- [33] J. Yousefi, "Image binarization using Otsu thresholding algorithm," *Ontario, Canada: University of Guelph*, pp. 1–4, 2011, doi: 10.13140/RG.2.1.4758.9284.
- [34] N. Zhu, G. Wang, G. Yang, and W. Dai, "A fast 2D Otsu thresholding algorithm based on improved histogram," in *2009 Chinese Conference on Pattern Recognition*, Nov. 2009, pp. 1–5, doi: 10.1109/CCPR.2009.5344078.
- [35] J. G. M. Schavemaker, M. J. T. Reinders, J. J. Gerbrands, and E. Backer, "Image sharpening by morphological filtering," *Pattern Recognition*, vol. 33, no. 6, pp. 997–1012, Jun. 2000, doi: 10.1016/S0031-3203(99)00160-0.
- [36] R. M. Haralick and L. G. Shapiro, *Computer and robot vision*, vol. 1. Addison-wesley Reading, 1992.
- [37] P. P. Acharjya, A. Sinha, S. Sarkar, S. Dey, and S. Ghosh, "A new approach of watershed algorithm using distance transform applied to image segmentation," *International Journal of Innovative Research in Computer and Communication Engineering*, vol. 1, no. 2, pp. 185–189, 2013.
- [38] J. B. T. M. Roerdink and A. Meijster, "The watershed transform: Definitions, algorithms and parallelization strategies," *Fundamenta Informaticae*, vol. 41, no. 1,2, pp. 187–228, 2000, doi: 10.3233/FI-2000-411207.
- [39] R. Beare and G. Lehmann, "The watershed transform in ITK - discussion and new developments," *The Insight Journal*, Jun. 2006, doi: 10.54294/If8u75.
- [40] A. Kornilov and I. Safonov, "An overview of watershed algorithm implementations in open source libraries," *Journal of Imaging*, vol. 4, no. 10, Oct. 2018, doi: 10.3390/jimaging4100123.
- [41] V. J. Gaikwad, "Marker-controlled watershed transform in digital mammogram segmentation," *International Journal for Research in Applied Science & Engineering*, vol. 3, no. 3, pp. 18–21, 2015.

BIOGRAPHIES OF AUTHORS



Kiran Malhari Napte    received the B.Eng. degree in electronics engineering from Pune University, India in 2010 and the Master of Engineering degrees in Electronics & Telecommunication from Pune University in 2014. Currently, he is an Assistant Professor at the Department of Electronics and Telecommunication Engineering, PimpriChinchwad College of Engineering and Research, Ravet, Pune. His research interests include medical image processing, signal processing, pattern recognition, power electronics and artificial intelligence in healthcare. He can be contacted at email: kiran.napte@pccoer.in.



Anurag Mahajan    received B.E. in Electronics Engineering from Vikram University, Ujjain in 1998. He received M.E. in Electronics and Communication Engineering from University of Roorkee, Roorkee (Now IIT, Roorkee) in 2000. He received Ph.D. from Jaypee University of Engineering and Technology, Guna in 2014. He worked in Medi-Caps Institute of Technology and Management, Indore in Electronics and Communication Engineering Department from August 2002 to January 2008 at different position from Lecturer to Reader. He worked as Assistant Professor in Jaypee University of Engineering and Technology, Guna in Electronics and Communication Engineering Department from January 2008 to December 2017. Presently he is working as Assistant Professor in Electronics and Telecommunication Engineering Department in Symbiosis Institute of Technology, Symbiosis International (Deemed University), Pune since December 2017. He can be contacted at email: anurag.mahajan@sitpune.edu.in.